Oxygen-specific photoelectron circular dichroism in gas-phase fenchone

Juliette Leroux,[1,2] Dominik Stemer,[3,*] Bruno Credidio,[3] Filippa Dudda,[2] Emilia Heikura,[4] Akhila Jose,[2] Alice Judt,[2,5] Catmarna Küstner-Wetekam,[4] Moritz Zander,[2] Nikolay M. Novikovskiy,[4] Thorsten Otto,[6] Parth Patil,[2,6] Gunnar Petersen,[2] Sara Savio,[2] Nicolas Velasquez,[3] Niclas Wieland,[2] Lasse Wülfing,[7] Philipp V. Demekhin,[4,†] Florian Trinter,[3,‡] and Markus Ilchen[2,6,§]

[1]*The Hamburg Centre for Ultrafast Imaging, 22761 Hamburg, Germany*
[2]*Department of Physics, Universität Hamburg, 22607 Hamburg, Germany*
[3]*Molecular Physics, Fritz-Haber-Institut der Max-Planck-Gesellschaft, 14195 Berlin, Germany*
[4]*Institut für Physik und CINSaT, Universität Kassel, 34132 Kassel, Germany*
[5]*European XFEL, 22869 Schenefeld, Germany*
[6]*Deutsches Elektronen-Synchrotron DESY, 22603 Hamburg, Germany*
[7]*Fakultät Physik, Technische Universität Dortmund, 44227 Dortmund, Germany*

(Received 27 October 2025; accepted 24 February 2026; published 30 March 2026)

Understanding the light-driven responses of chiral molecular systems at a fundamental level—electronically—via photoelectron circular dichroism (PECD) provides a pathway to unlock the intricate mechanisms governing the functionality of chiral molecules. The specific role of oxygen atoms in chiral compounds remains under-explored, despite their pivotal role in numerous functional systems. We report a joint experimental and theoretical study of the PECD of O 1*s* electrons from the randomly oriented chiral molecule fenchone ($C_{10}H_{16}O$) in the gas phase across a kinetic-energy range from 3 to 15 eV. We observe a substantial forward-backward asymmetry in the electron emission patterns across several eV, which is well reproduced by relaxed-core Hartree-Fock calculations. Our results provide a site-specific perspective on the chiral sensitivity of an oxygen atom directly connected to the stereocenter of a chiral molecule.

DOI: 10.1103/cgf3-cdpv

I. INTRODUCTION

Chirality plays a fundamental role in biology, chemistry, and physics, particularly in living organisms, where amino acids and sugars exist exclusively as single enantiomers, i.e., nonsuperimposable mirror images [1,2]. Although enantiomers share almost identical physical properties, they interact differently with other chiral objects or phenomena, such as circularly polarized light. Because enantiomers interact differently with other chiral molecules, the chemical activity of molecules *in vivo* can differ significantly between enantiomers. For this reason, the ability to distinguish between enantiomers is critical in pharmaceutical research [3].

Circularly polarized light is a powerful tool for investigating chiral molecules in the gas phase, as it carries the required intrinsic handedness to interact with a chiral molecule dichroically, i.e., show a distinct difference between the interaction with left-(LCP) and right-circularly polarized (RCP) light. The helicity dependence of light-matter interaction can thus offer the sensitivity to discriminate enantiomers and is commonly referred to as circular dichroism. An even stronger effect than the simple photoabsorption difference of opposing helicities can be achieved for the so-called photoelectron circular dichroism (PECD) [4]. Ritchie first theorized PECD in 1976 [5], showing that, for chiral molecules, the photoelectron angular emission distribution exhibits a forward-backward asymmetry with respect to the direction of the light propagation. Importantly, this asymmetry inverts upon exchanging either the molecular enantiomer or the light's helicity. This prediction was experimentally confirmed by Böwering *et al.* in 2001, who recorded PECD in the angular distribution of randomly oriented gas-phase bromocamphor [6]. Since PECD is a pure electric-dipole effect, its magnitude can substantially exceed that of conventional circular dichroism, i.e., the photon-absorption-yield difference between the helicities of the light [7–11], and the effect is considered universal across the photoionization regimes.

The PECD effect for randomly oriented molecules typically reaches up to a few percent, depending on electron kinetic energy and the system under investigation [10,12–15]. It has been both observed and predicted that, in the soft x-ray range, PECD magnitudes of electrons emitted from localized orbitals are similarly strong and can, in exceptional cases, even approach 20%, as demonstrated for fenchone at the carbon K-edge [16]. PECD in the soft x-ray regime thus

*Present address: Physikalisches Institut, Universität Münster, 48149, Münster.
†Contact author: demekhin@physik.uni-kassel.de
‡Contact author: trinter@fhi-berlin.mpg.de
§Contact author: markus.ilchen@uni-hamburg.de

Published by the American Physical Society under the terms of the Creative Commons Attribution 4.0 International license. Further distribution of this work must maintain attribution to the author(s) and the published article's title, journal citation, and DOI.

provides not only a powerful but also an element-specific probe for chirality [16–18]. PECD at the oxygen K-edge, in particular, offers an intriguing perspective on element- and thus site-specific sensitivity regarding direct prospects for intermolecular chiral processes, such as hydration effects and dynamics. Despite this rich scientific potential, PECD measurements at the oxygen K-edge remain scarce [19–24].

Fenchone is an ideal candidate for PECD studies due to its rigid structure, which ensures the presence of a single conformer even at room temperature, and its extensive use as a prototypical system in both experimental and theoretical work [11,13,18,25–37]. The molecular structure of fenchone is shown as an inset in Fig. 2(c). Its PECD response in the gas phase was first measured at the carbon K-edge by Ulrich *et al.* [16] and subsequently verified by Malerz *et al.* [38], while liquid-phase fenchone PECD has been measured at the carbon K-edge by Pohl *et al.* [39]. Since fenchone contains only one oxygen atom, oxygen K-edge PECD studies are particularly insightful, as the effect can be unambiguously assigned to a single atomic site in the molecule.

In this study, we apply soft x-ray radiation to investigate the PECD of gas-phase fenchone at the oxygen K-edge. We determine the strength of the asymmetric electron emission patterns, i.e., the forward-backward asymmetry, imprinted onto its oxygen core-shell electrons, in order to benchmark the effect and site-specifically determine the chiral sensitivity of the oxygen atom in fenchone.

II. EXPERIMENTAL METHODS

The PECD experiments were performed at the P04 soft x-ray beamline of the PETRA III synchrotron (DESY, Hamburg, Germany) [40], using the EASI (Electronic structure of Aqueous Solutions and Interfaces) setup as previously described [38]. PETRA III operates in a top-up operation mode at 120 mA in multibunch mode, ensuring ideal beam stability over time. Beamline P04 provides a high photon flux of up to several 10^{12} photons/s at a resolving power of up to 10^4. The EASI setup is designed to perform PECD experiments in both the liquid and gas phases. In brief, it combines a state-of-the-art, differentially pumped ambient-pressure hemispherical electron analyzer with either a liquid jet mount for liquid-phase experiments or a simple gas target for gas-phase measurements [38].

Photoelectrons from the fenchone O 1*s* state, between ≈3 and 15 eV kinetic energy (i.e., 541–553 eV nominal photon energy with an uncertainty of ±0.3 eV), were detected in the backward direction, with the electron analyzer mounted at an angle of 130° with respect to the light propagation axis [38]. The photoelectron spectra at 545 eV photon energy, for both light polarizations, of R-(–)-fenchone are shown in Fig. 1. This approximates the magic-angle geometry of 125.26°, where all possible electron angular distribution anisotropies are equal, while accounting for the geometrical constraints of the open port of the beamline [38,41–43]. The P04 beamline is equipped with an APPLE-II undulator, which provides a high degree of circular polarization of (97 ± 3)% [22,44–51]. Prior to the PECD measurements, we recorded undulator profiles by scanning the monochromator energy at fixed undulator gap and shift settings to ensure that the photon energy and beam intensity are the same for both helicities. The helicity was switched every 15 min between left- [positive (+) helicity] and right-handed [negative (−) helicity] circular polarizations to ensure equal experimental conditions for the two cases. We used a laminar 1200 lines/mm (9 nm groove depth) grating and an exit-slit opening of 100 μm, resulting in 75 meV photon-energy resolution and a focus of 180 μm (horizontal) × 35 μm (vertical). The employed energy resolution of the electron analyzer was 40 meV using a pass energy of 20 eV. This results in a combined energy resolution of 85 meV for both the photon energy and the electron analyzer.

Both enantiomers of fenchone were purchased from Sigma-Aldrich with a chemical purity of ⩾98% and used without further purification. For both enantiomers, liquid fenchone was placed in a reservoir outside the vacuum chamber and introduced effusively into the interaction region through a 1.5 mm diameter stainless steel nozzle. The fenchone vapor was then ionized by the circularly polarized light. Photoelectrons passing through a 0.8 mm diameter skimmer cone were energetically resolved in the hemispherical electron analyzer by spatial dispersion. To ensure a stable partial pressure (total pressure of 2×10^{-5} mbar in the main vacuum chamber), the sample reservoir was placed in a water bath maintained at approximately 35°C. Furthermore, to prevent cross-contamination with the other enantiomer, the injection line and sample reservoir were completely replaced between measurements of the two different enantiomers.

Moreover, we performed regular control measurements at 575 eV photon energy to monitor our experimental conditions over time, as no PECD signal is expected at this photon energy. The PECD measurements were performed in the order of +, −, −, and + undulator shifts to minimize errors due to changes in target density over the timescale of hours.

Data treatment

To process the data recorded during this experimental campaign, we used an in-house script developed by Stemer *et al.* for aqueous-phase alanine [52]. Each pair of O 1*s* photoelectron spectra of fenchone (one measurement performed with left-handed circularly polarized light and one with right-handed circularly polarized light; see Fig. 1 for an exemplary set at 545 eV photon energy) resulted from averaging five individual spectral acquisitions. As slight energy offsets of 5–10 meV were observed between measurements, an energetic correction was performed by aligning the O 1*s* peak features of each pair of spectra prior to analysis. Each pair of spectra was then normalized in intensity, using the achiral background signal as a reference. This procedure served to correct for slight remnant differences in photon flux between the two light polarizations (2%–3%). Unlike in the previous work on aqueous-phase alanine [52], background subtraction for gas-phase fenchone was more straightforward and was performed using a polynomial fit over the measured kinetic-energy range. The asymmetry factor [see Eq. (2) below] of gas-phase fenchone at the O K-edge was then extracted from the processed data. The percent difference was calculated pointwise between the spectra and summed within the peak of interest to yield a single value of PECD per measurement

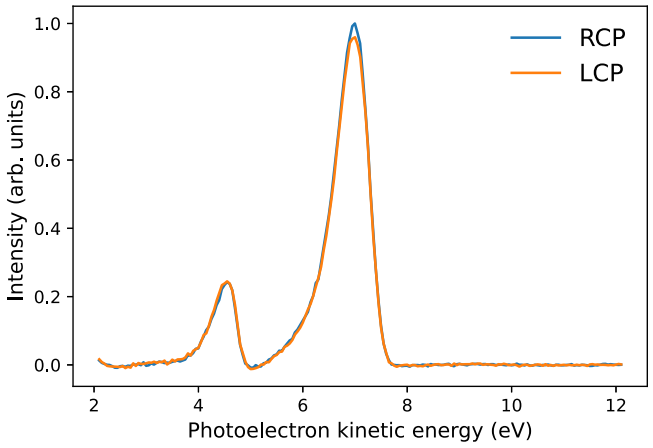


FIG. 1. Background-subtracted photoelectron spectra recorded for both light polarizations at 545 eV photon energy for R-(–)-fenchone. The first peak, at approximately 4.5 eV kinetic energy, originates from the residual gas, whereas the feature at 6.9 eV kinetic energy corresponds to the characteristic O 1*s* photoelectron peak of fenchone.

pair. Each datapoint corresponds to two to four measurement pairs. All data reduction was performed using the Igor Pro analysis software (WaveMetrics, version 9).

For randomly oriented molecules, the normalized photoelectron angular distribution under the electric-dipole approximation [4,5] is given by

$$I^{\pm}(\theta) = 1 \pm b_1 P_1(\cos\theta) - \tfrac{1}{2} b_2 P_2(\cos\theta). \tag{1}$$

Here, $I^{\pm}(\theta)$ is the photoionization intensity at an angle θ, measured with respect to the propagation direction of the photon beam for circularly polarized light with (+) or (−) helicity, and b_1 and b_2 are the dichroic and anisotropy angular distribution parameters, respectively. From this, we extract the asymmetry factor, defined as the difference between photoelectron yields, recorded with the left- and right-handed circularly polarized light, normalized to their average, such as

$$G = \frac{I^+ - I^-}{\frac{1}{2}(I^+ + I^-)} = \frac{2b_1 \cos\theta}{1 - \frac{1}{2} b_2 P_2(\cos\theta)}. \tag{2}$$

This asymmetry factor provides access to b_1, which describes the PECD effect. However, it requires knowledge of b_2. Since our detection was performed at $\theta = 130°$, i.e., close to the magic angle, we approximate the term $P_2(\cos\theta) \approx 0$ [38,39,52]. This leads to

$$b_1 = \frac{I^+ - I^-}{I^+ + I^-} \frac{1}{\cos(130°)}. \tag{3}$$

Due to the geometrical constraints of the P04 beamline, we operate at this near-magic angle of 130°, where $P_2(\cos(130°)) \neq 0$. Therefore, the b_2 parameter has some influence on the b_1 parameter. Unfortunately, we were unable to experimentally determine b_2 due to the constraints of the setup as described above. As previously done [39,52], using our calculations, we can estimate an upper limit for the b_2 contribution on the measured b_1 parameter. The calculations suggest that for the kinetic-energy range covered in our experiment (i.e., 3–15 eV), b_2 lies between 0.4 and 1.2 [see Fig. 2(c)]. Considering the acceptance angle of the electron analyzer (approximately ±15°), the residual effect on b_1 would correspond to scaling factors of 0.967 (for $b_2 = 0.4$) and 0.958 (for $b_2 = 1.2$). This correction does not significantly impact the extracted b_1 (approximately 3%–4% error on the value) and was therefore included in the given uncertainty.

We finally note that we report here the dichroic parameter b_1, as shown in Fig. 2(b), and not the PECD, which is equal to $2b_1$ [4,15,29].

III. THEORETICAL METHODS

The present calculations of O 1*s* photoionization in fenchone were carried out using the stationary single-center method [53–55], similar to our previous studies on the outer-shell ionization of this molecule [33,34,37]. Briefly, the calculations were performed at the equilibrium internuclear geometry of the ground electronic state of neutral R-(–)-fenchone, within the relaxed-core Hartree-Fock approximation (see below for details). The bound occupied molecular orbitals of the neutral and core-ionized molecule were generated using the PC GAMESS (US) [56] quantum chemistry package with a triplet zeta valence (TZV) basis set [57], augmented by two additional *p*-type and one *d*-type polarization functions. These orbitals were represented by single-center expansions, restricted to angular momentum quantum numbers ℓ, $|m| \leqslant 99$, and further used to generate the direct and exchange electronic potentials for the photoelectron in the continuum and to calculate the respective photoionization transition amplitudes.

The partial photoelectron continuum waves, with angular momentum quantum numbers ℓ, $|m| \leqslant 29$, were computed in the ionic potential, which includes the monopole relaxation of the ionic orbitals due to the O 1*s* core vacancy created by the photoionization. The core relaxation was modeled in the present work in the equivalent-core approximation using a fractional nuclear charge for the core-ionized atom [58,59]. In particular, the bound occupied molecular orbitals, used to generate the electronic potential for the photoelectron provided by the singly core-ionized molecule, were computed in the molecule with all 84 electrons but using the nuclear charge of 8.5 assigned to the oxygen atom. Thereby, all molecular orbitals relax in the presence of an additional fractional point charge of +0.5 (optimized in Refs. [58,59] for the near-threshold C 1*s* photoionization of the CO molecule), as if half of the well-localized, photoionized core electron were missing. The explicit equations used to calculate the dichroic and anisotropy parameters from the photoionization transition amplitudes can be found in Refs. [19,60].

The calculations were performed in the photoelectron energy range of 1–15 eV in steps of 2 eV and further spline interpolated in steps of 0.1 eV. The present computational results are depicted in Fig. 2 and made publicly available (see "Data availability" statement).

IV. RESULTS AND DISCUSSION

In Fig. 1, the averaged background-subtracted photoelectron spectra of R-(–)-fenchone at the photon energy of 545 eV for both light polarizations are shown. We observe a main

O 1*s* peak at 6.9 eV kinetic energy originating from the fenchone carbonyl group, with an additional lower-energy peak due to residual gas in the interaction chamber. Because the fenchone O 1*s* peak and the contaminant peak do not overlap, the dichroic parameter b_1 can still be extracted in a straightforward manner.

The calculated photoionization cross section of the fenchone O 1*s* orbital is displayed in Fig. 2(a) and drops from about 0.58 to 0.39 Mb in the energy range of investigation. This result is very different than the cross section of the fenchone C 1*s* orbital calculated by Ulrich *et al.* [16], where they found that the cross section oscillates between 0.8 and 3 Mb in the 3–15 eV kinetic-energy range. However, this is in agreement with the experimental cross section of CO_2 at the O 1*s* edge that oscillates between 0.8 and 0.6 Mb in the same kinetic-energy range [61].

Using the employed electron spectrometer and beamline monochromator, from the photoelectron spectrum at each photon energy, we can derive an O 1*s* binding energy of gaseous fenchone of (538.1 ± 0.5) eV. Note that the error originates from both the spectrometer and the monochromator.

The analysis of photoelectron spectra in the low-kinetic-energy range of 3–15 eV is particularly relevant, as this energy window exhibits strong sensitivity to electronic and structural chirality features near the ionization threshold. Therefore, in Fig. 2(b), the experimental dichroic parameter b_1 for S-(+)- and R-(–)-fenchone is shown as a function of photoelectron kinetic energy in this range, together with the calculated values.

As expected, we observe an almost mirror-symmetric behavior between the two enantiomers, with a sizable b_1 value between ≈ 4 and 10 eV and a reduction of its magnitude to less than a percent at the lower and higher energies. The experimental dichroic parameter exhibits two sign inversions over the measured kinetic-energy range: one at about 3 eV and one at higher kinetic energies (above 12 eV). This, however, remains ambiguous within the reported uncertainty. Notably, theory predicts this inversion only for the higher-energy part.

For the S-(+)-enantiomer, b_1 reaches a maximum of $\sim +4.1\%$ at ≈ 5 eV kinetic energy. This is not supported by the corresponding measurements for the R-(–)-enantiomer, which give a b_1 value of $\sim -2.2\%$ at this kinetic energy. Moreover, for R(–)-fenchone, b_1 reaches a maximum value of $\sim -2.7\%$ at ≈ 7 eV kinetic energy, which is agreeing with the theoretical value within the given uncertainty.

Overall, our theoretical calculations are in very good agreement with the experimental results. Over the investigated photoelectron energy range, the theoretical dichroic parameter follows the same trend as the measured value, with the strongest b_1 of 3.8% at ≈ 5 eV kinetic energy.

Interestingly, the sign of the PECD observed for O 1*s* ionization in fenchone is opposite to that previously reported for carbonyl C 1*s* ionization by Ulrich *et al.* [16], with the ionized atoms in these studies being direct neighbors. Since the molecular structure is identical and only the vista of interrogation of the chiral response via PECD is slightly altered, this sign change [32,62] reflects the sensitivity of the photoelectron scattering process to the local molecular environment. It thus indicates that the formation mechanisms of the PECD are highly site specific and represent a complex interplay between electronic states and the chiral molecular structure [10]. Moreover, the asymmetry in the O 1*s* photoemission is reduced by around half in comparison with its measured asymmetry at the C 1*s* edge [16], where the authors showed that, for the R-(–)-enantiomer, its b_1 value reaches $\sim +8\%$ at 5 eV kinetic energy. This b_1 value decreases between 8 and 15 eV and reaches $\sim +2\%$ while remaining positive throughout the measured kinetic-energy range [16].

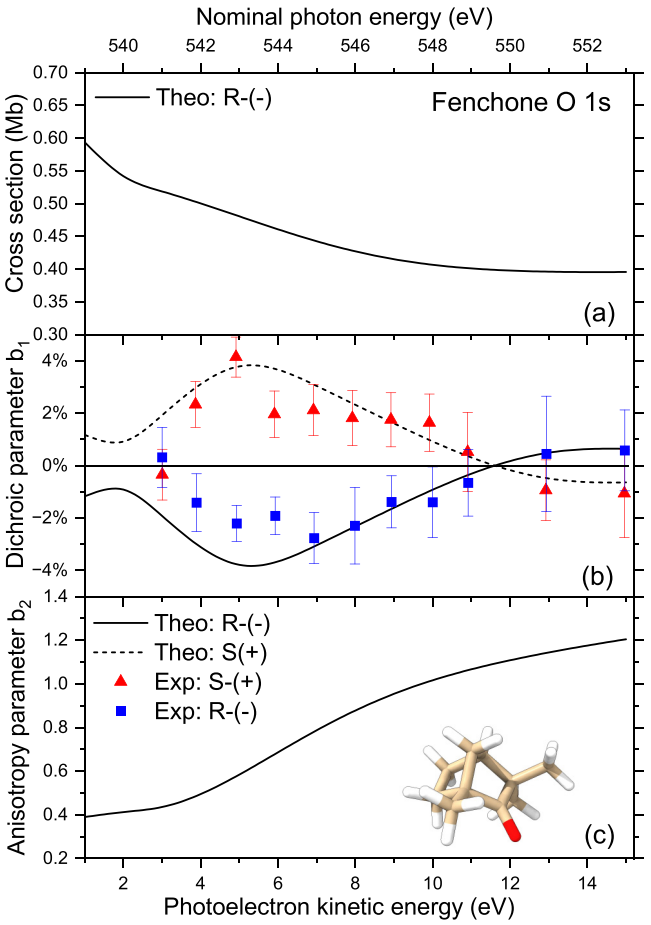


FIG. 2. (a) Computed photoionization cross section. (b) Dichroic parameter b_1, measured for (R)-(–)-fenchone (blue) and S-(+)-fenchone (red), with their calculated error bars overlapped with the computed parameters of R-(–)-fenchone (solid curve) and S-(+)-fenchone (dashed curve). (c) The computed anisotropy parameter b_2 is shown together with the molecular structure of fenchone (PubChem ID 14525).

As shown in Eq. (2), our estimation of the asymmetry factor G depends on the anisotropy parameter b_2. Although our experimental geometry does not allow for a b_2 determination, the calculation provides an estimate of b_2 and enables us to derive a potential error for the b_1 parameter as described above. The calculated anisotropy parameter b_2 is shown in Fig. 2(c). It varies significantly, from 0.4 to 1.2, in the kinetic-energy range of this study, which, beyond providing access to accurate scaling factors, can be an interesting perspective for future studies. A more detailed analysis of the b_2

parameters can provide deeper insight into the orbital structures underlying the asymmetric angular distribution patterns in chiral molecules, particularly under resonance conditions, and, in this regard, the most relevant energy region just above the ionization threshold.

V. CONCLUSIONS AND OUTLOOK

We have measured core-level photoelectron circular dichroism at the oxygen K-edge for the two enantiomers of gas-phase fenchone using the EASI setup at the P04 beamline of the PETRA III synchrotron. In addition to the experimental finding of the PECD for O 1*s* electrons of fenchone, we reported an estimate for its O 1*s* binding energy. We presented calculations of the photoionization cross section as well as the dichroic and anisotropy angular distribution parameters in the range from 1 to 15 eV kinetic energy. This study represents one of the first demonstrations of PECD at the oxygen K-edge in randomly oriented gas-phase systems, providing valuable references for future investigations of the general role of oxygen in chiral media and intermolecular effects in, e.g., microhydration. Extending these measurements to a broader range of small molecules will advance the development of a comprehensive PECD database at the oxygen 1*s* core level. In the future, we aim to build on our findings of a sizable oxygen-specific PECD in order to conduct ultrafast, time-resolved PECD measurements on gas-phase molecules using x-ray free-electron lasers, which offer unique advantages in this regard. Pump-probe experiments could directly track changes in the chiral electronic environment around the oxygen atom following electronic excitation or molecular dissociation, offering detailed insights into chiral dynamics at the atomic level. These approaches could also be extended to nanosolvated systems, allowing for the exploration of how water molecules influence molecular chirality and electronic properties during ultrafast processes. Investigating such effects may yield critical insights into the role of hydration in shaping biomolecular chirality, with implications for understanding biological function and stereochemical behavior.

ACKNOWLEDGMENTS

This work was supported/funded by the Cluster of Excellence "CUI: Advanced Imaging of Matter" of the Deutsche Forschungsgemeinschaft (DFG)—EXC 2056—Project ID 390715994. We acknowledge DESY (Hamburg, Germany), a member of the Helmholtz Association HGF, for the provision of experimental facilities. Parts of this research were carried out at PETRA III, and we would like to thank Moritz Hoesch and his team for assistance in using beamline P04. Beamtime was allocated for Proposal No. H-20010092. The calculations were supported in part through the Maxwell computational resources operated at DESY. D.S. acknowledges funding from the European Research Council under the European Union's Horizon 2020 research and innovation program—Grant No. GAP 883759-AQUACHIRAL. N.M.N. and P.V.D. acknowledge support from the Deutsche Forschungsgemeinschaft (DFG)—Project No. 328961117—SFB 1319 ELCH (Extreme light for sensing and driving molecular chirality). N.V. and F.T. acknowledge funding by the Deutsche Forschungsgemeinschaft (DFG, German Research Foundation)—Project No. 509471550, Emmy Noether Programme. The molecular graphic was performed with UCSF ChimeraX, developed by the Resource for Biocomputing, Visualization, and Informatics at the University of California, San Francisco [63].

DATA AVAILABILITY

The data that support the findings of this article are openly available [64].

[1] E. Babaev, D. Kharzeev, M. Larsson, A. Molochkov, and V. Zhaunerchyk, Chiral matter, in *Proceedings of the Nobel Symposium 167* (World Scientific, 2023).

[2] Y. Liu, Z. Wu, D. W. Armstrong, H. Wolosker, and Y. Zheng, Detection and analysis of chiral molecules as disease biomarkers, Nat. Rev. Chem. **7**, 355 (2023).

[3] J. Ceramella, D. Iacopetta, A. Franchini, M. De Luca, C. Saturnino, I. Andreu, M. S. Sinicropi, and A. Catalano, A look at the importance of chirality in drug activity: Some significative examples, Appl. Sci. **12**, 10909 (2022).

[4] M. H. M. Janssen and I. Powis, Detecting chirality in molecules by imaging photoelectron circular dichroism, Phys. Chem. Chem. Phys. **16**, 856 (2014).

[5] B. Ritchie, Theory of the angular distribution for ejection of photoelectrons from optically active molecules and molecular negative ions. II, Phys. Rev. A **14**, 359 (1976).

[6] N. Böwering, T. Lischke, B. Schmidtke, N. Müller, T. Khalil, and U. Heinzmann, Asymmetry in photoelectron emission from chiral molecules induced by circularly polarized light, Phys. Rev. Lett. **86**, 1187 (2001).

[7] U. Boesl von Grafenstein and A. Bornschlegl, Circular dichroism laser mass spectrometry: Differentiation of 3-methylcyclopentanone enantiomers, ChemPhysChem **7**, 2085 (2006).

[8] A. I. S. Holm, L. M. Nielsen, S. V. Hoffmann, and S. B. Nielsen, Vacuum-ultraviolet circular dichroism spectroscopy of DNA: A valuable tool to elucidate topology and electronic coupling in DNA, Phys. Chem. Chem. Phys. **12**, 9581 (2010).

[9] U. J. Meierhenrich, J.-J. Filippi, C. Meinert, J. H. Bredehöft, J.-i. Takahashi, L. Nahon, N. C. Jones, and S. V. Hoffmann, Circular dichroism of amino acids in the vacuum-ultraviolet region, Angew. Chem. Int. Ed. **49**, 7799 (2010).

[10] M. Wollenhaupt, Photoelectron circular dichroism in different ionization regimes, New J. Phys. **18**, 121001 (2016).

[11] S. Beaulieu, A. Comby, D. Descamps, B. Fabre, G. A. Garcia, R. Géneaux, A. G. Harvey, F. Légaré, Z. Mašín, L. Nahon, A. F. Ordonez, S. Petit, B. Pons, Y. Mairesse, O. Smirnova, and V. Blanchet, Photoexcitation circular dichroism in chiral molecules, Nat. Phys. **14**, 484 (2018).

[12] I. Powis, Photoelectron circular dichroism of the randomly oriented chiral molecules glyceraldehyde and lactic acid, J. Chem. Phys. **112**, 301 (2000).

[13] C. Lux, M. Wollenhaupt, T. Bolze, Q. Liang, J. Köhler, C. Sarpe, and T. Baumert, Circular dichroism in the photoelectron angular distributions of camphor and fenchone from multiphoton ionization with femtosecond laser pulses, Angew. Chem. Int. Ed. **51**, 5001 (2012).

[14] C. S. Lehmann, N. B. Ram, I. Powis, and M. H. M. Janssen, Imaging photoelectron circular dichroism of chiral molecules by femtosecond multiphoton coincidence detection, J. Chem. Phys. **139**, 234307 (2013).

[15] L. Nahon, G. A. Garcia, and I. Powis, Valence shell one-photon photoelectron circular dichroism in chiral systems, J. Electron Spectrosc. Relat. Phenom. **204**, 322 (2015).

[16] V. Ulrich, S. Barth, S. Joshi, U. Hergenhahn, E. Mikajlo, C. J. Harding, and I. Powis, Giant chiral asymmetry in the C 1 s core level photoemission from randomly oriented fenchone enantiomers, J. Phys. Chem. A **112**, 3544 (2008).

[17] M. Ilchen *et al.*, Site-specific interrogation of an ionic chiral fragment during photolysis using an x-ray free-electron laser, Commun. Chem. **4**, 119 (2021).

[18] D. Faccialà *et al.*, Time-resolved chiral x-ray photoelectron spectroscopy with transiently enhanced atomic site selectivity: A free-electron laser investigation of electronically excited fenchone enantiomers, Phys. Rev. X **13**, 011044 (2023).

[19] M. Ilchen, G. Hartmann, P. Rupprecht, A. N. Artemyev, R. N. Coffee, Z. Li, H. Ohldag, H. Ogasawara, T. Osipov, D. Ray, P. Schmidt, T. J. A. Wolf, A. Ehresmann, S. Moeller, A. Knie, and P. V. Demekhin, Emitter-site-selective photoelectron circular dichroism of trifluoromethyloxirane, Phys. Rev. A **95**, 053423 (2017).

[20] M. Tia *et al.*, Observation of enhanced chiral asymmetries in the inner-shell photoionization of uniaxially oriented methyloxirane enantiomers, J. Phys. Chem. Lett. **8**, 2780 (2017).

[21] K. Fehre *et al.*, Fourfold differential photoelectron circular dichroism, Phys. Rev. Lett. **127**, 103201 (2021).

[22] G. Nalin *et al.*, Photoelectron circular dichroism of O 1*s*-photoelectrons of uniaxially oriented trifluoromethyloxirane: Energy dependence and sensitivity to molecular configuration, Phys. Chem. Chem. Phys. **23**, 17248 (2021).

[23] K. Fehre, F. Trinter, N. M. Novikovskiy, S. Grundmann, D. Tsitsonis, S. Eckart, L. Bauer, M. Hilzinger, T. Jahnke, R. Dörner, P. V. Demekhin, and M. S. Schöffler, Influence of the emission site on the photoelectron circular dichroism in trifluoromethyloxirane, Phys. Chem. Chem. Phys. **24**, 13597 (2022).

[24] G. Nalin *et al.*, Molecular-frame differential photoelectron circular dichroism of O 1*s*-photoelectrons of trifluoromethyloxirane, Phys. Rev. Res. **5**, 013021 (2023).

[25] F. J. Devlin, P. J. Stephens, J. R. Cheeseman, and M. J. Frisch, *Ab initio* prediction of vibrational absorption and circular dichroism spectra of chiral natural products using density functional theory: Camphor and fenchone, J. Phys. Chem. A **101**, 6322 (1997).

[26] G. Longhi, S. Abbate, R. Gangemi, E. Giorgio, and C. Rosini, Fenchone, camphor, 2-methylenefenchone and 2-methylenecamphor: A vibrational circular dichroism study, J. Phys. Chem. A **110**, 4958 (2006).

[27] M. Stener, D. Di Tommaso, G. Fronzoni, P. Decleva, and I. Powis, Theoretical study on the circular dichroism in core and valence photoelectron angular distributions of camphor enantiomers, J. Chem. Phys. **124**, 024326 (2006).

[28] I. Powis, C. J. Harding, G. A. Garcia, and L. Nahon, A valence photoelectron imaging investigation of chiral asymmetry in the photoionization of fenchone and camphor, ChemPhysChem **9**, 475 (2008).

[29] C. Lux, M. Wollenhaupt, C. Sarpe, and T. Baumert, Photoelectron circular dichroism of bicyclic ketones from multiphoton ionization with femtosecond laser pulses, ChemPhysChem **16**, 115 (2015).

[30] A. Comby, S. Beaulieu, M. Boggio-Pasqua, D. Descamps, F. Légaré, L. Nahon, S. Petit, B. Pons, B. Fabre, Y. Mairesse, and V. Blanchet, Relaxation dynamics in photoexcited chiral molecules studied by time-resolved photoelectron circular dichroism: Toward chiral femtochemistry, J. Phys. Chem. Lett. **7**, 4514 (2016).

[31] L. Nahon, L. Nag, G. A. Garcia, I. Myrgorodska, U. Meierhenrich, S. Beaulieu, V. Wanie, V. Blanchet, R. Géneaux, and I. Powis, Determination of accurate electron chiral asymmetries in fenchone and camphor in the VUV range: Sensitivity to isomerism and enantiomeric purity, Phys. Chem. Chem. Phys. **18**, 12696 (2016).

[32] A. Kastner, T. Ring, B. C. Krüger, G. B. Park, T. Schäfer, A. Senftleben, and T. Baumert, Intermediate state dependence of the photoelectron circular dichroism of fenchone observed via femtosecond resonance-enhanced multi-photon ionization, J. Chem. Phys. **147**, 013926 (2017).

[33] A. D. Müller, A. N. Artemyev, and P. V. Demekhin, Photoelectron circular dichroism in the multiphoton ionization by short laser pulses. II. Three- and four-photon ionization of fenchone and camphor, J. Chem. Phys. **148**, 214307 (2018).

[34] A. D. Müller, E. Kutscher, A. N. Artemyev, and P. V. Demekhin, Photoelectron circular dichroism in the multiphoton ionization by short laser pulses. III. Photoionization of fenchone in different regimes, J. Chem. Phys. **152**, 044302 (2020).

[35] V. Blanchet, D. Descamps, S. Petit, Y. Mairesse, B. Pons, and B. Fabre, Ultrafast relaxation investigated by photoelectron circular dichroism: An isomeric comparison of camphor and fenchone, Phys. Chem. Chem. Phys. **23**, 25612 (2021).

[36] D. P. Singh, J. O. F. Thompson, K. L. Reid, and I. Powis, Influence of vibrational excitation and nuclear dynamics in multiphoton photoelectron circular dichroism of fenchone, J. Phys. Chem. Lett. **12**, 11438 (2021).

[37] E. Kutscher, A. N. Artemyev, and P. V. Demekhin, Photoelectron circular dichroism in fenchone by short coherent broadband laser pulses, Phys. Rev. A **107**, 013107 (2023).

[38] S. Malerz, H. Haak, F. Trinter, A. B. Stephansen, C. Kolbeck, M. Pohl, U. Hergenhahn, G. Meijer, and B. Winter, A setup for studies of photoelectron circular dichroism from chiral molecules in aqueous solution, Rev. Sci. Instrum. **93**, 015101 (2022).

[39] M. N. Pohl, S. Malerz, F. Trinter, C. Lee, C. Kolbeck, I. Wilkinson, S. Thürmer, D. M. Neumark, L. Nahon, I. Powis, G. Meijer, B. Winter, and U. Hergenhahn, Photoelectron circular dichroism in angle-resolved photoemission from liquid fenchone, Phys. Chem. Chem. Phys. **24**, 8081 (2022).

[40] J. Viefhaus, F. Scholz, S. Deinert, L. Glaser, M. Ilchen, J. Seltmann, P. Walter, and F. Siewert, The variable polarization XUV beamline P04 at PETRA III: Optics, mechanics and their

performance, Nucl. Instrum. Methods Phys. Res. Sect. A **710**, 151 (2013).

[41] J. Feldhaus, W. Erlebach, A. L. D. Kilcoyne, K. J. Randall, and M. Schmidbauer, An angle-resolving photoelectron spectrometer for the simultaneous measurement of cross sections and asymmetry parameters using synchrotron radiation, Rev. Sci. Instrum. **63**, 1454 (1992).

[42] A. Giardini, D. Catone, S. Stranges, M. Satta, M. Tacconi, S. Piccirillo, S. Turchini, N. Zema, G. Contini, T. Prosperi, P. Decleva, D. Di Tommaso, G. Fronzoni, M. Stener, A. Filippi, and M. Speranza, Angle-resolved photoelectron spectroscopy of randomly oriented 3-hydroxytetrahydrofuran enantiomers, ChemPhysChem **6**, 1164 (2005).

[43] D. J. H. Cant, B. P. Reed, B. F. Spencer, W. R. Flavell, and A. G. Shard, Magic angle HAXPES, J. Electron Spectrosc. Relat. Phenom. **264**, 147311 (2023).

[44] G. Hartmann, M. Ilchen, P. Schmidt, C. Küstner-Wetekam, C. Ozga, F. Scholz, J. Buck, F. Trinter, J. Viefhaus, A. Ehresmann, M. S. Schöffler, A. Knie, and P. V. Demekhin, Recovery of high-energy photoelectron circular dichroism through Fano interference, Phys. Rev. Lett. **123**, 043202 (2019).

[45] L. Kaiser, K. Fehre, N. M. Novikovskiy, J. Stindl, D. Tsitsonis, G. Gopakumar, I. Unger, J. Söderström, O. Björneholm, M. Schöffler, T. Jahnke, R. Dörner, F. Trinter, and P. V. Demekhin, Angular emission distribution of O 1*s* photoelectrons of uniaxially oriented methanol, J. Phys. B: At. Mol. Opt. Phys. **53**, 194002 (2020).

[46] A. Pier, K. Fehre, S. Grundmann, I. Vela-Perez, N. Strenger, M. Kircher, D. Tsitsonis, J. B. Williams, A. Senftleben, T. Baumert, M. S. Schöffler, P. V. Demekhin, F. Trinter, T. Jahnke, and R. Dörner, Chiral photoelectron angular distributions from ionization of achiral atomic and molecular species, Phys. Rev. Res. **2**, 033209 (2020).

[47] D. V. Rezvan, K. Klyssek, S. Grundmann, A. Pier, N. M. Novikovskiy, N. Strenger, D. Tsitsonis, M. Kircher, I. Vela-Peréz, K. Fehre, F. Trinter, M. S. Schöffler, T. Jahnke, R. Dörner, and P. V. Demekhin, Observation of nondipole-induced asymmetry in the angular emission distribution of photoelectrons from fixed-in-space CO molecules, Phys. Rev. Lett. **129**, 253201 (2022).

[48] D. V. Rezvan, A. Pier, S. Grundmann, N. M. Novikovskiy, N. Anders, M. Kircher, N. Melzer, F. Trinter, M. S. Schöffler, T. Jahnke, R. Dörner, and P. V. Demekhin, Nondipolar photoelectron angular distributions from fixed-in-space N_2 molecules, J. Phys. B: At. Mol. Opt. Phys. **57**, 145101 (2024).

[49] D. Tsitsonis, F. Trinter, J. B. Williams, K. Fehre, P. V. Demekhin, T. Jahnke, R. Dörner, and M. S. Schöffler, Enantioselective one-photon excitation of formic acid, Phys. Rev. Lett. **133**, 093002 (2024).

[50] S. S. Brinkman, X. L. Tan, B. Brekke, A. C. Mathisen, Ø. Finnseth, R. J. Schenk, K. Hagiwara, M.-J. Huang, J. Buck, M. Kalläne, M. Hoesch, K. Rossnagel, K.-H. Ou Yang, M.-T. Lin, G.-J. Shu, Y.-J. Chen, C. Tusche, and H. Bentmann, Chirality-driven orbital angular momentum and circular dichroism in CoSi, Phys. Rev. Lett. **132**, 196402 (2024).

[51] J. Schusser, H. Orio, M. Ünzelmann, J. Heßdörfer, M. P. T. Masilamani, F. Diekmann, K. Rossnagel, and F. Reinert, Towards robust dichroism in angle-resolved photoemission, Commun. Phys. **7**, 270 (2024).

[52] D. Stemer, S. Thürmer, F. Trinter, U. Hergenhahn, M. Pugini, B. Credidio, S. Malerz, I. Wilkinson, L. Nahon, G. Meijer, I. Powis, and B. Winter, Photoelectron circular dichroism of aqueous-phase alanine, Chem. Sci. **16**, 8637 (2025).

[53] P. V. Demekhin, A. Ehresmann, and V. L. Sukhorukov, Single center method: A computational tool for ionization and electronic excitation studies of molecules, J. Chem. Phys. **134**, 024113 (2011).

[54] S. A. Galitskiy, A. N. Artemyev, K. Jänkälä, B. M. Lagutin, and P. V. Demekhin, Hartree-Fock calculation of the differential photoionization cross sections of small Li clusters, J. Chem. Phys. **142**, 034306 (2015).

[55] N. M. Novikovskiy, A. N. Artemyev, D. V. Rezvan, B. M. Lagutin, and P. V. Demekhin, Multichannel single center method, J. Phys. B: At. Mol. Opt. Phys. **55**, 175001 (2022).

[56] M. W. Schmidt, K. K. Baldridge, J. A. Boatz, S. T. Elbert, M. S. Gordon, J. H. Jensen, S. Koseki, N. Matsunaga, K. A. Nguyen, S. Su, T. L. Windus, M. Dupuis, and J. A. Montgomery, Jr., General atomic and molecular electronic structure system, J. Comput. Chem. **14**, 1347 (1993).

[57] T. H. Dunning, Jr., Gaussian Basis Functions for Use in Molecular Calculations. III. Contraction of (10s6p) Atomic Basis Sets for the First-Row Atoms, J. Chem. Phys. **55**, 716 (1971).

[58] N. A. Cherepkov, S. K. Semenov, A. V. Golovin, J. Adachi, and A. Yagishita, O K-shell photoemission of the CO molecule: Comparison between theory and experiment, J. Phys. B: At. Mol. Opt. Phys. **37**, 4803 (2004).

[59] S. K. Semenov, N. A. Cherepkov, T. Jahnke, and R. Dörner, Theoretical study of vibrationally resolved photoionization for the C K-shell of the CO molecule, J. Phys. B: At. Mol. Opt. Phys. **37**, 1331 (2004).

[60] A. Knie, M. Ilchen, P. Schmidt, P. Reiß, C. Ozga, B. Kambs, A. Hans, N. Müglich, S. A. Galitskiy, L. Glaser, P. Walter, J. Viefhaus, A. Ehresmann, and P. V. Demekhin, Angle-resolved study of resonant Auger decay and fluorescence emission processes after core excitations of the terminal and central nitrogen atoms in N_2O, Phys. Rev. A **90**, 013416 (2014).

[61] K. Maier, A. Kivimäki, B. Kempgens, U. Hergenhahn, M. Neeb, A. Rüdel, M. N. Piancastelli, and A. M. Bradshaw, Influence of multielectron excitations on the O 1*s* photoionization in CO_2, Phys. Rev. A **58**, 3654 (1998).

[62] K. Fehre, S. Eckart, M. Kunitski, C. Janke, D. Trabert, J. Rist, M. Weller, A. Hartung, L. P. H. Schmidt, T. Jahnke, R. Dörner, and M. Schöffler, Link between photoelectron circular dichroism and fragmentation channel in strong field ionization, J. Phys. Chem. A **123**, 6491 (2019).

[63] E. F. Pettersen, T. D. Goddard, C. C. Huang, E. C. Meng, G. S. Couch, T. I. Croll, J. H. Morris, and T. E. Ferrin, UCSF ChimeraX: Structure visualization for researchers, educators, and developers, Protein Sci. **30**, 70 (2021).

[64] J. Leroux, Oxygen-specific photoelectron circular dichroism in gas-phase fenchone [Data set], Zenodo (2026), https://doi.org/10.5281/zenodo.15648896.